

# LONG-BASELINE NEUTRINO OSCILLATIONS <sup>1</sup>

*Stephen J. PARKE*

Fermi National Accelerator Laboratory  
P.O. Box 500, Batavia, IL 60510, U.S.A.

## Abstract

A systematic study of potential long-baseline (distances  $>300$  km) neutrino oscillation experiments performed with  $\nu_\mu$  and  $\bar{\nu}_\mu$  beams from the new Fermilab Main Injector ( $\langle E_\nu \rangle \approx 10\text{--}20$  GeV) is presented. The effects of matter enhancement are included if the oscillation is into the electron neutrino channel. We find that there are three key variables for such an experiment, the length of the baseline, the charged lepton energy threshold and the minimum measurable oscillation probability. An advantage in one of these variables can easily be negated by a disadvantage in one of the others. Finally, for any long-baseline experiment at these energies to conclusively confirm or refute the interpretation of the atmospheric neutrino deficit as neutrino oscillations it must have a low energy threshold and a low minimum measurable oscillation probability.

## 1 Introduction

The recent indications of a deficit in the  $\nu_\mu$  flux of atmospheric neutrinos and the long-standing solar neutrino problem have motivated new searches for neutrino oscillations with small neutrino  $\Delta m^2$  ( $< 1\text{eV}^2$ ).<sup>[1]</sup> The neutrino beams available from the Fermilab Main Injector<sup>[2]</sup> will provide a unique laboratory for the study of such effects. They will be intense, well-understood beams with neutrino energies from 10–50 GeV and by constructing experiments at large distances (hundreds of kilometers) the experiments can probe regions of parameter space relevant to these puzzles. One feature of such experiments is that the neutrino beams would pass through the Earth's crust, permitting matter-enhancement to affect the oscillations. This paper addresses the physics accessible at such experiments and many details and references can be found in ref.[3].

---

<sup>1</sup>Invited talk at the "15<sup>th</sup> Johns Hopkins Workshop" August 26-28, 1991 at Johns Hopkins University, Baltimore, MD.

## 2 Review of Oscillation Phenomenology

### 2.1 Review of Neutrino Oscillations in Vacuum

The time evolution of an ultra-relativistic plane wave neutrino state propagating in vacuum with momentum  $K$  in the mass eigenstate basis is given by the trivial relation:

$$|\nu(t)\rangle = \nu_1^0(t) |\nu_1^0\rangle + \nu_2^0(t) |\nu_2^0\rangle. \quad (2.1)$$

The Dirac equation for this state reduces to the following Schrodinger-like equation:

$$i \frac{d}{dt} \begin{pmatrix} \nu_1^0 \\ \nu_2^0 \end{pmatrix} = \begin{pmatrix} \sqrt{K^2 + m_1^2} & 0 \\ 0 & \sqrt{K^2 + m_2^2} \end{pmatrix} \begin{pmatrix} \nu_1^0 \\ \nu_2^0 \end{pmatrix}. \quad (2.2)$$

In the ultra-relativistic limit we can use the approximation that

$$\sqrt{K^2 + m_i^2} = \left( K + \frac{m_1^2 + m_2^2}{4K} \right) \mp \frac{\Delta m_0^2}{4K} + \mathcal{O}\left(\frac{m^4}{K^3}\right) \quad (2.3)$$

where  $\Delta m_0^2 \equiv m_2^2 - m_1^2$  and the minus (plus) sign is for the 1 (2) eigenstate. Notice that in this expression  $\left( K + \frac{m_1^2 + m_2^2}{4K} \right)$  is common to both mass eigenstates and can be removed by changing the overall phase of the neutrino state by an amount

$$\exp\left( i \left( K + \frac{m_1^2 + m_2^2}{4K} \right) t \right). \quad (2.4)$$

After this change of phase the time evolution is governed by

$$i \frac{d}{dt} \begin{pmatrix} \nu_1^0 \\ \nu_2^0 \end{pmatrix} = \frac{1}{2} \begin{pmatrix} -\frac{\Delta m_0^2}{2K} & 0 \\ 0 & \frac{\Delta m_0^2}{2K} \end{pmatrix} \begin{pmatrix} \nu_1^0 \\ \nu_2^0 \end{pmatrix}. \quad (2.5)$$

In general the vacuum mass eigenstates are not identical to the flavor eigenstates but are related by

$$\begin{pmatrix} \nu_1^0 \\ \nu_2^0 \end{pmatrix} = \begin{pmatrix} \cos \theta_0 & \sin \theta_0 \\ -\sin \theta_0 & \cos \theta_0 \end{pmatrix} \begin{pmatrix} \nu_e \\ \nu_\mu \end{pmatrix}, \quad (2.6)$$

where  $\theta_0$  is the vacuum mixing angle. In this flavor basis the time evolution is

$$i \frac{d}{dt} \begin{pmatrix} \nu_e \\ \nu_\mu \end{pmatrix} = \frac{1}{2} \begin{pmatrix} -\frac{\Delta m_0^2}{2K} \cos 2\theta_0 & \frac{\Delta m_0^2}{2K} \sin 2\theta_0 \\ \frac{\Delta m_0^2}{2K} \sin 2\theta_0 & \frac{\Delta m_0^2}{2K} \cos 2\theta_0 \end{pmatrix} \begin{pmatrix} \nu_e \\ \nu_\mu \end{pmatrix}. \quad (2.7)$$

From Eqs. 2.5 and 2.6 it is easy to calculate the probability of producing one flavor of neutrino  $\nu_a$  at the source, letting the neutrino propagate to the detector,

a distance  $L$  away, and then detecting the neutrino as a different flavor  $\nu_b$ . This transition probability is

$$\mathcal{P}_{ab} = \sin^2 2\theta_0 \sin^2 \left( 1.27 \frac{\Delta m_0^2 L}{K} \right) \quad (2.8)$$

where  $\Delta m_0^2$ ,  $K$  and  $L$  are measured in  $\text{eV}^2$ ,  $\text{GeV}$ , and kilometers respectively (we use these units throughout). The experiments measure this probability and either measure a finite value for  $\mathcal{P}_{ab}$  or assign a limit  $\mathcal{P}_{ab} < P_{min}$ ; the value of  $P_{min}$ , the energy spectrum of detected neutrinos and the source–detector distance then define a region in the  $(\sin^2 2\theta_0, \Delta m_0^2)$  plane for each experiment. This  $P_{min}$  is the minimum measurable oscillation probability for the experiment in a given analysis mode.

The size of  $P_{min}$ , or the limit in our ability to measure  $\mathcal{P}_{ab}$ , arises from four sources (assuming the statistical errors are small compared to the systematic uncertainties): (1) the contamination of the beam with other neutrino species, (2) the fractional uncertainty in the neutrino flux calculations, (3) the knowledge of the experimental acceptance for the different neutrino species, and (4) backgrounds to the  $\nu_b$  signal. Then for large  $\Delta m_0^2$  an experiment can explore any

$$\sin^2 2\theta_0 \geq 2 P_{min}. \quad (2.9)$$

The factor of two comes from averaging the  $\sin^2 (1.27 \Delta m_0^2 L / K)$  term in Eq. 2.8.

For  $\sin^2 2\theta_0 = 1$  the limit on the mass difference squared is

$$\Delta m_0^2 \geq \frac{\sqrt{P_{min}} K}{1.27 L}, \quad (2.10)$$

assuming  $P_{min} \ll 1$ . Note the momentum factor in the numerator as this will be important to us later. For smaller  $\sin^2 2\theta_0$  a good *approximation* to the probability contour is a straight line with slope  $-1/2$  in a log-log plot in the  $(\sin^2 2\theta_0, \Delta m_0^2)$  plane until this line intersects the vertical line from Eq. 2.9. In Fig. 1a this region is shown for a neutrino momentum of 30  $\text{GeV}$  with  $L = 6000 \text{ km}$  and  $P_{min} = 3\%$ .

## 2.2 Neutrino Oscillations in Matter

The effect of matter on the neutrino evolution is seen easily in the flavor basis. The electron neutrino can elastically forward scatter off the electrons in the matter through the charged current interaction<sup>[4]</sup> whereas the muon neutrinos cannot. The term that must be added to the top diagonal element of the evolution matrix in Eq. 2.7 is<sup>[5]</sup>

$$+ \sqrt{2} G_F N_e. \quad (2.11)$$

Once again it is convenient to make the diagonal elements of the evolution matrix equal in magnitude but opposite in sign by changing the overall phase of the neutrino

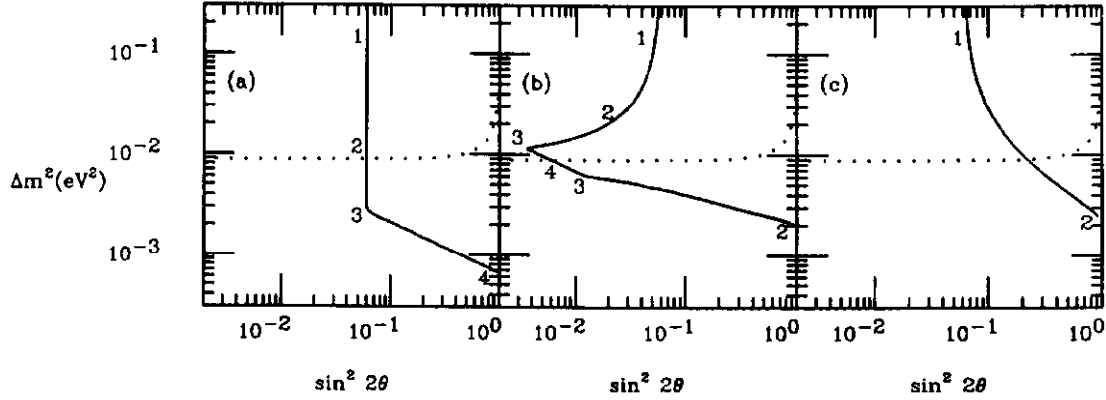


Figure 1: For a 30 GeV neutrino beam the solid curve represents the parameter range accessible for a 6000 km experiment with  $P_{min} = 3\%$ . Part (a) is the vacuum experiment using the variables  $(\sin^2 2\theta_0, \Delta m_0^2)$  or the matter experiment in the variables  $(\sin^2 2\theta_N, \Delta m_N^2)$ . Fig. (b) is the matter experiment in the variables  $(\sin^2 2\theta_0, \Delta m_0^2)$  and (c) is the same as (b) but for an antineutrino beam. The dotted curve is explained in the text.

state by

$$\exp\left(i \frac{G_F N_e t}{\sqrt{2}}\right). \quad (2.12)$$

Then the neutrino evolution equation becomes

$$i \frac{d}{dt} \begin{pmatrix} \nu_e \\ \nu_\mu \end{pmatrix} = \frac{1}{2} \begin{pmatrix} -\frac{\Delta m_0^2}{2K} \cos 2\theta_0 + \sqrt{2} G_F N_e & \frac{\Delta m_0^2}{2K} \sin 2\theta_0 \\ \frac{\Delta m_0^2}{2K} \sin 2\theta_0 & \frac{\Delta m_0^2}{2K} \cos 2\theta_0 - \sqrt{2} G_F N_e \end{pmatrix} \begin{pmatrix} \nu_e \\ \nu_\mu \end{pmatrix}. \quad (2.13)$$

If  $N_e$  is a constant or simple function this evolution equation can be solved analytically; otherwise it must be integrated numerically.

For uniform matter the matter mass eigenstates are the natural basis. They are obtained by finding  $\Delta m_N^2$  and  $\theta_N$  such that

$$\begin{aligned} \frac{\Delta m_N^2}{2K} \cos 2\theta_N &= \frac{\Delta m_0^2}{2K} \cos 2\theta_0 - \sqrt{2} G_F N_e \\ \frac{\Delta m_N^2}{2K} \sin 2\theta_N &= \frac{\Delta m_0^2}{2K} \sin 2\theta_0, \end{aligned} \quad (2.14)$$

where  $\theta_N$  is the matter mixing angle that determines the matter mass eigenstates in terms of the flavor eigenstates:

$$\begin{pmatrix} \nu_1^N \\ \nu_2^N \end{pmatrix} = \begin{pmatrix} \cos \theta_N & \sin \theta_N \\ -\sin \theta_N & \cos \theta_N \end{pmatrix} \begin{pmatrix} \nu_e \\ \nu_\mu \end{pmatrix}, \quad (2.15)$$

The resonance density is the density which makes the diagonal elements of Eq. 2.13 zero and hence maximally mixes the two neutrino species,

$$\theta_N = \frac{\pi}{4} \quad (2.16)$$

and

$$N_e = \frac{\Delta m_o^2 \cos 2\theta_o}{2K\sqrt{2}G_F}. \quad (2.17)$$

The time evolution in terms of these mass eigenstates is:

$$i \frac{d}{dt} \begin{pmatrix} \nu_1^N \\ \nu_2^N \end{pmatrix} = \frac{1}{2} \begin{pmatrix} -\frac{\Delta m_N^2}{2K} & 0 \\ 0 & \frac{\Delta m_N^2}{2K} \end{pmatrix} \begin{pmatrix} \nu_1^N \\ \nu_2^N \end{pmatrix}. \quad (2.18)$$

From Eqs. 2.15 and 2.18 it is easy to see that the form of the transition probability is the same as before (Eq. 2.8), but with the matter angles and matter mass difference squared replacing their vacuum values:

$$\mathcal{P}_{ab} = \sin^2 2\theta_N \sin^2 \left( 1.27 \frac{\Delta m_N^2 L}{K} \right). \quad (2.19)$$

In terms of these matter parameters,  $(\sin^2 2\theta_N, \Delta m_N^2)$  the limits on the experiment are the same as before:

$$\sin^2 2\theta_N \geq 2 P_{min} \quad (2.20)$$

and

$$\Delta m_N^2 \geq \frac{\sqrt{P_{min}} K}{1.27 L}. \quad (2.21)$$

In terms of the  $(\sin^2 2\theta_0, \Delta m_0^2)$  plane we have to use Eq. 2.14 to make the transformation between the two. This is straightforward except in the case that  $\cos 2\theta_N$  is negative. This occurs when the number density of electrons is larger than the resonance density of Eq. 2.17. Fig. 1b is what happens to the region of Fig. 1a if we assume  $\nu_\mu \leftrightarrow \nu_e$  oscillations using an average  $Y_e \rho = 1.9 \text{ gcm}^{-3}$  and  $L = 6000 \text{ km}$ . Starting at the top of the figure using  $\cos 2\theta_N > 0$  then the points 1 thru 4 in Figs. 1a map into the corresponding points in Fig. 1b. Similarly the points 4 to 2 in

Fig. 1a with  $\cos 2\theta_N < 0$  map out the lower section labelled 4 to 2 in Fig. 1b. The dotted line in these figures is the condition  $\Delta m^2 \cos 2\theta = 2K \sqrt{2}G_F N_e$ .

If we fix the detector distance  $L$  and the minimum measurable probability  $P_{min}$  but vary the momentum  $K$  the plot is scaled up or down without any change in shape. This is because the bulge on the left of the plot is caused by the mass difference being close to the value needed for resonance

$$\Delta m_0^2 = \frac{2K \sqrt{2}G_F N_e}{\cos 2\theta_0}. \quad (2.22)$$

This  $\Delta m_0^2$  scales with momentum in exactly the same way as does the minimum  $\Delta m_0^2$  of Eq. 2.10. The size of the bulge is determined by the distance between the source and the detector and the number density of electrons in the mantle of the Earth.

### 2.3 Anti-Neutrino Oscillation Experiments in Matter

For anti-neutrinos propagating through matter, the situation is the same as for neutrinos but with

$$\sqrt{2}G_F N_e \longrightarrow -\sqrt{2}G_F N_e. \quad (2.23)$$

Fig. 1c is the same as Fig. 1b except for anti-neutrinos instead of neutrinos where  $\cos 2\theta_N$  is always greater than zero. We have implicitly assumed  $\Delta m_0^2$  is positive; if it is negative then the roles of neutrinos and anti-neutrinos are reversed.

## 3 Results and Conclusions

A detailed evaluation of the systematic errors in long-baseline oscillation experiments is beyond the scope of this paper. Our approach has been to assume a minimum measurable oscillation probability,  $P_{min}$ , and calculate the attainable limits.  $P_{min}$  will vary within the same experiment depending on the method used to determine if oscillations are present, from disappearance to appearance experiments in the same detector and between detectors.

We have calculated the limits with  $\nu_\mu$  and  $\bar{\nu}_\mu$  spectra given in ref.[2]. The neutrinos and anti-neutrinos then produced charged leptons through charged-current interactions using the appropriate  $y$ -distribution for deep-inelastic scattering.<sup>[7]</sup>

The acceptance for charged leptons is a complicated and experiment-dependent quantity. We modeled it with a  $\theta$ -function; if the charged lepton energy was less than 5, 10, or 20 GeV (each of three cases) the charged lepton was considered lost; for energies greater than the appropriate value the acceptance was assumed perfect. For this analysis the hadron shower was assumed to be unobservable. The neutrinos oscillated according to Eq. 2.13 and a grid of probabilities was then calculated, leading

to the contours. We have included the effects of the varying density of the Earth<sup>[6]</sup> by integrating this equation over the chords of interest;  $\Delta\rho/\rho < 15\%$  and the effects are small when compared with the constant density approximation.

We first present the results for  $\nu_\mu \leftrightarrow \nu_\tau$  oscillations. Since these oscillations are unaffected by matter-enhancement, the contours scale in a simple way. We plot  $\nu_\mu \leftrightarrow \nu_\tau$  contours at 600 and 6000 km for  $P_{min} = 1\%$ , 3%, and 10% in Figs. 2 and 3 for neutrinos and anti-neutrinos respectively. These figures are very similar but differ slightly due to different spectra and y-distributions for the neutrinos and anti-neutrinos.

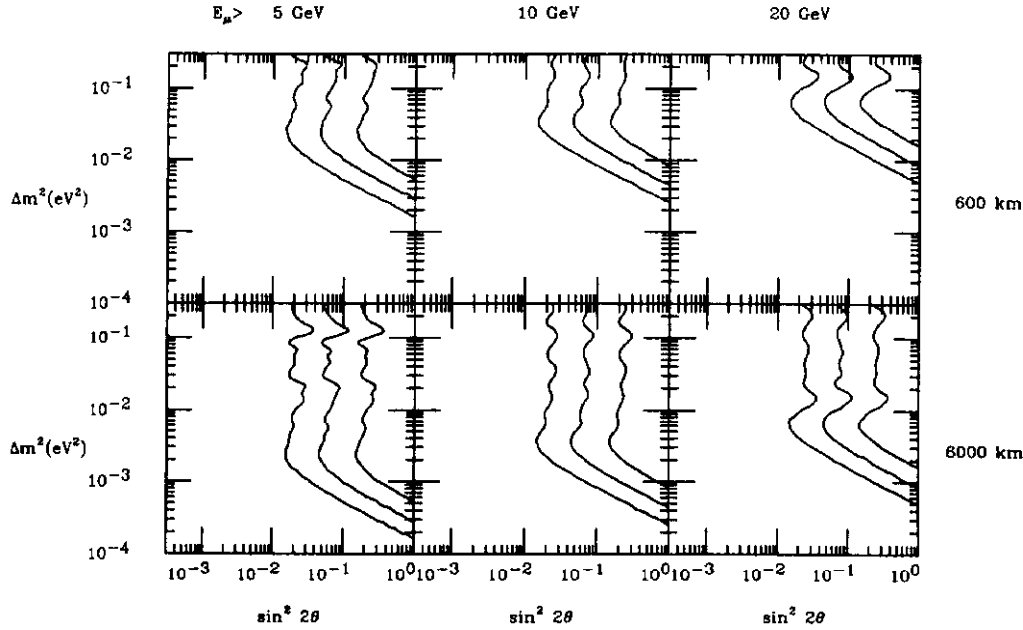


Figure 2: The excluded region in the  $(\sin^2 2\theta_0, \Delta m_0^2)$  plane for  $\nu_\mu \leftrightarrow \nu_\tau$  for  $L = 600$  and 6000 km with  $P_{min} = 1, 3$  and 10% and muon-detection thresholds as shown.

The results for  $\nu_\mu \leftrightarrow \nu_e$  oscillations at 600 and 6000 km are shown in Fig. 4 for neutrinos and Fig. 5 for anti-neutrinos. We see immediately that for a given experiment the region of sensitivity is enlarged due to matter enhancement for neutrinos and reduced by matter enhancement for anti-neutrinos. Both of these effects could be investigated in an appropriate experiment. However, the statistics of an anti-neutrino run would suffer from the smaller cross-section ( $\sigma_{\bar{\nu}}/\sigma_\nu \approx 0.5$ ) and from a less intense  $\bar{\nu}_\mu$  beam; hence an anti-neutrino experiment would need to run for six times as long as its neutrino counterpart to achieve the same statistical power.

There are a number of proposals<sup>[8]</sup> to do a long baseline search using a new neutrino beam from the Fermilab new main injector. Any of these experiments would

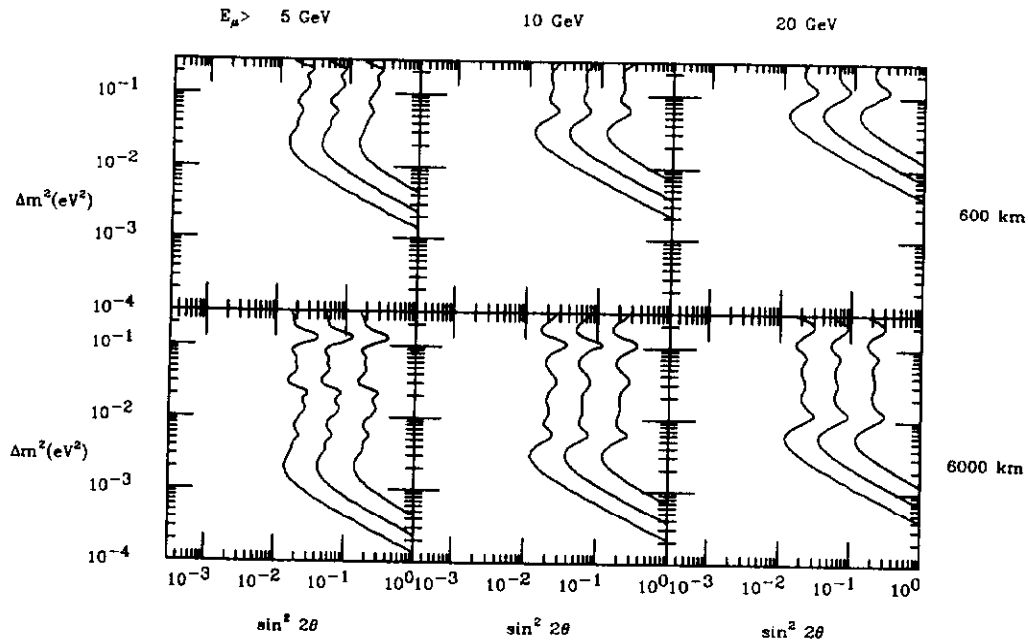


Figure 3: The excluded region in the  $(\sin^2 2\theta_0, \Delta m_0^2)$  plane for  $\bar{\nu}_\mu \leftrightarrow \bar{\nu}_\tau$  for  $L = 600$  and  $6000$  km with  $P_{min} = 1, 3$  and  $10\%$  and muon-detection thresholds as shown. This plot is marginally different from Fig. 2 because of the different  $y$ -distributions and spectra for neutrinos and anti-neutrinos.

clearly confirm or refute the neutrino oscillation hypothesis as the cause of the atmospheric neutrino result. The region favored by this hypothesis is  $\Delta m_{\mu\tau}^2 \sim 0.03 \text{ eV}^2$  with a large mixing angle,<sup>[9]</sup> well within the sensitive regions discussed here.

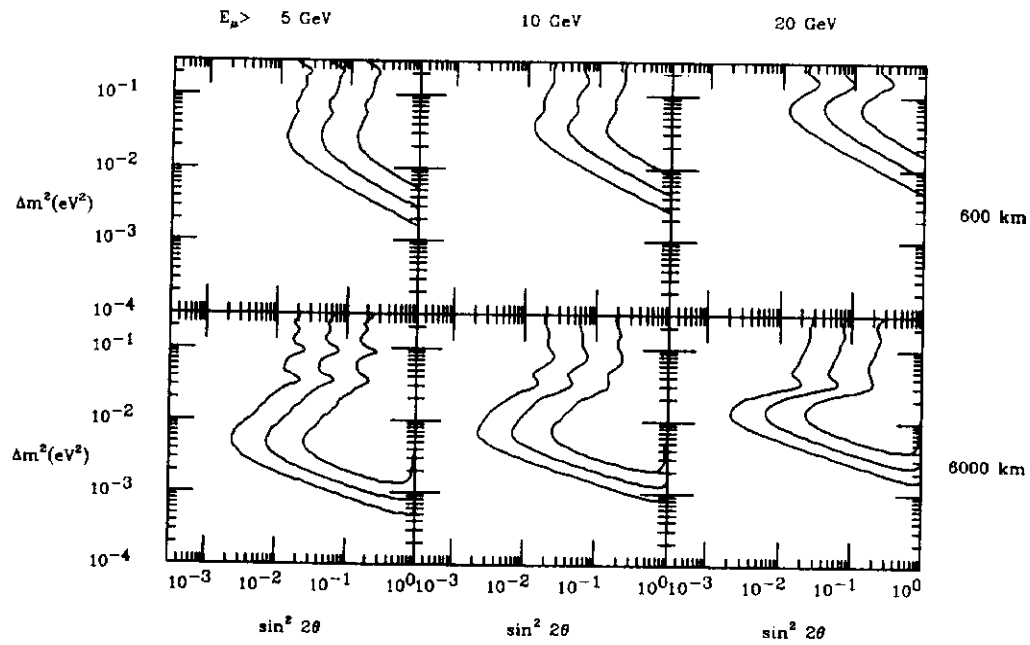


Figure 4: The exclusion region in the  $(\sin^2 2\theta_0, \Delta m_0^2)$  plane for  $\nu_\mu \leftrightarrow \nu_e$  oscillations in the Earth for  $L = 600$  and  $6000$  km with  $P_{min} = 1, 3,$  and  $10\%$  and muon-detection thresholds as shown.

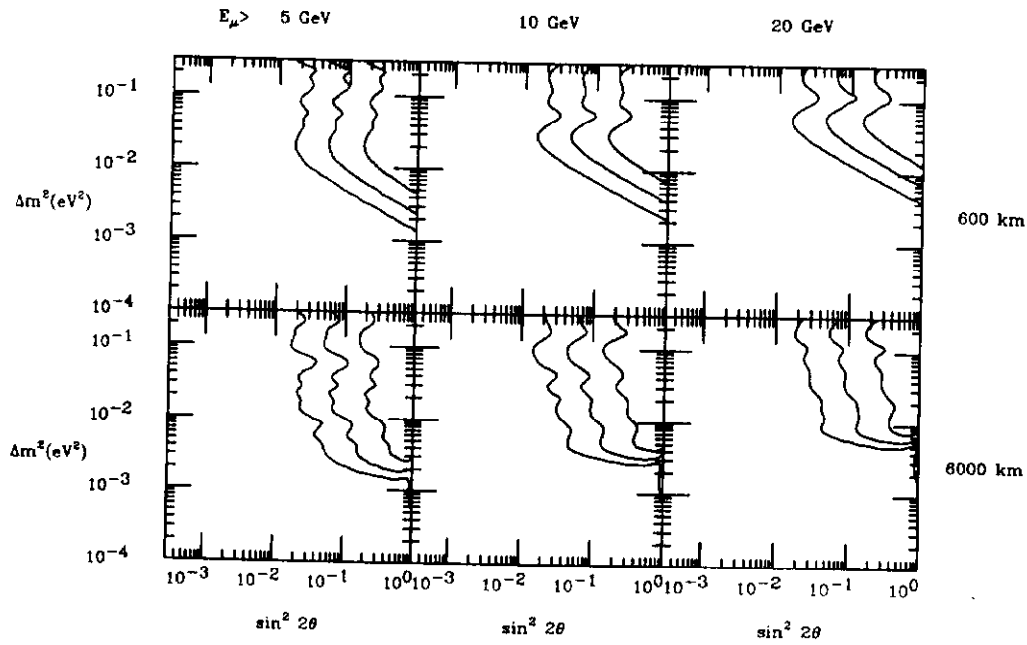


Figure 5: The exclusion region in the  $(\sin^2 2\theta_0, \Delta m_0^2)$  plane for  $\bar{\nu}_\mu \leftrightarrow \bar{\nu}_e$  oscillations in the Earth for  $L = 600$  and  $6000$  km with  $P_{min} = 1, 3,$  and  $10\%$  and muon-detection thresholds as shown.

## 4 Acknowledgements

I would like to thank R. H. Bernstein for his contributions to this work. Fermilab is operated by the Universities Research Association Inc. under contract with the United States Department of Energy.

## References

- [1] K. S. Hirata, *et al.*, Experimental Study of the Atmospheric Neutrino Flux, *Phys. Lett.* **205B** 416, (1988); T. Kajita, in *Singapore '90*, (World Scientific), to be published; D. Casper *et al.*, "Measurement of Atmospheric Neutrino Composition with IMB", BU preprint 90-23, (1990), submitted to *Phys. Rev. Lett.*; Ch. Berger, *et al.*, *Phys. Lett.* **245B** 305, (1990); Ch. Berger, *et al.*, *Phys. Lett.* **B227** 489 (1989); M. Aglietta, *et al.*, *Europhys. Lett.* **8** 611 (1989); M. Takita, University of Tokyo Ph.D. Thesis (1989); R. Davis *et al.*, *Phys. Rev. Lett.* **20** 1205, (1968).
- [2] Conceptual Design Report: The Fermilab Main Injector, Rev. 2.3, FNAL, April, 1990 (unpublished); R. Bernstein *et al.*, Conceptual Design Report: Neutrino Physics after the Main Injector Upgrade, FNAL, 1991 (unpublished).
- [3] R. H. Bernstein and S. J. Parke, Fermilab-Pub-91/59-T, March 1991. To be published in *Phys. Rev. D*, () .
- [4] There is also a flavor diagonal contribution from the neutral current interaction which can be removed by an overall phase change.
- [5] L. Wolfenstein, *Phys. Rev.* **D17** 2369, (1978).
- [6] See, for example, F. D. Stacey, *Physics of the Earth*, (Wiley, New York, 1969).
- [7] The structure functions were obtained by the CCFR collaboration. See E. Oltman, Nevis Pub. #270, Ph.D. Thesis (unpublished).
- [8] K. Kodama *et al.*, Muon Neutrino to Tau Neutrino Oscillations, FNAL Proposal P-803; W. Gajewski *et al.*, A Proposal for a Long Baseline Oscillation Experiment Using a High Intensity Neutrino Beam from the Fermilab Main Injector to the IMB Water Cerenkov Detector, FNAL Proposal P-805; W. Allison *et al.*, A Long Baseline Neutrino Oscillation Experiment Using Soudan 2, FNAL Proposal P-822; DUMAND-II Collaboration, A Terrestrial Long-Baseline Neutrino Oscillation Experiment using the Proposed Fermilab Main Injector and the DUMAND Detector, FNAL Proposal P-824.
- [9] J. Learned, S. Pakvasa, and T. Weiler, *Phys. Lett.* **207B** 79, (1988).